High-energy square-wave pulses generated in a 1/1.5-μm dual-band mode-locked fiber laser

Yihuai Zhu,[1] Jiachen Wang,[1] Weiqi Liu,[1] Geguo Du,[2] Shuangchen Ruan,[1] Chunyu Guo,[1] Peiguang Yan,[1] Ping Hua,[3] Linzhong Xia,[4] and Qitao Lue[5]

[1]Shenzhen Key Laboratory of Laser Engineering, Key Laboratory of Advanced Optical Precision Manufacturing Technology of Guangdong Higher Education Institutes, Guangdong Provincial Key Laboratory of Micro/Nano Optomechatronics Engineering, College of Physics and Optoelectronic Engineering, Shenzhen University, Shenzhen 518060, China
[2]College of Electronics and Information Engineering, Shenzhen University, Shenzhen 518060, China
[3]Faculty of Engineering and Physical Sciences, University of Southampton, Southampton SO171BJ, UK
[4]Shenzhen Institute of Information Technology, Shenzhen 518172, China
[5]Han's Laser Technology Industry Group Co., Ltd., Shenzhen 518057, China

Corresponding author: Chunyu Guo (e-mail: cyguo@szu.edu.cn)

Abstract: We experimentally demonstrated the generation of square-wave pulses in a 1/1.5-μm dual-band mode-locked fiber laser. The laser is based upon a peculiar "figure-θ" architecture that exploits a single active fiber to realize dual-band operation. High-energy square-wave pulses are simultaneously generated in both the 1-μm and the 1.5-μm spectral band using the laser. The pulses in both bands experience the extension of durations without the variation in peak amplitudes as the pump power is raised, and thus, the pulse energies can be continuously boosted. The 1-μm pulse maintains wave-breaking-free operation during the increase of the pump power and finally achieves an energy as high as 88.6 nJ, whilst the 1.5-μm pulse achieves an energy up to 1.5 μJ before it ultimately collapses into second-order mode-locking. To the best of our knowledge, this is the first report on the formation of square-wave pulse in dual-band mode-locked fiber lasers.

Index Terms: Fiber lasers, Dual-wavelength lasers, Mode-locked lasers.

1. Introduction

Owing to their cost-effectiveness, compactness, and high performance, mode-locked fiber lasers are intensely studied in the past decades as tools for a range of scientific and industrial applications. Various techniques such as nonlinear polarization rotation (NPR) [1], nonlinear amplifier loop mirror (NALM) [2], saturable absorbers [3]–[8], and active mode-locking [9] have been developed to realize mode-locking in fiber laser systems. In recent years, there is a growing interest in dual-band mode-locked fiber lasers, in which the optical pulses are generated in two distinct spectral bands simultaneously. Such lasers are attractive for versatile applications such as nonlinear frequency conversion, pump-probe process, and Raman spectroscopy [10], [11]. The development of such systems is challenging, in view of that the dual-band operation usually requires complicated systems [12]–[14].

Hitherto most reported dual-band mode-locked fiber lasers operate with low pulse energies. Common pulse species such as soliton, stretched pulse, dissipative soliton, and self-similar pulse [15]–[18] are limited on their pulse energies, or the pulses will split or convert into higher-order mode-locking. A probable solution for this issue is to introduce non-conventional pulses. Recently, square-wave pulses with rectangular profiles attract great attention [19]–[22]. The durations of square-wave pulses increase almost indefinitely as the pulse energies are raised, during which the pulses are free of splitting and the peak amplitudes of the pulses stay unchanged. Consequently, the pulse energies of square-wave pulses can reach levels much higher than conventional pulses.

In this paper, the generation of square-wave pulses in a dual-band mode-locked fiber laser is demonstrated. The laser employs a "figure-θ" configuration that utilizes a single active fiber to realize dual-band operation. Two-color square-wave pulses are generated from the laser in the 1-μm and the 1.5-μm band simultaneously. The maximum energies are 88.6 nJ for the 1-μm pulse and 1.5 μJ for the 1.5-μm pulse, respectively, which set the record of the pulse energies achieved using dual-band mode-locked fiber lasers. Such a high-energy performance can be merit for a number of applications.

2. Experimental setup

The schematic of the dual-band mode-locked fiber laser is shown in Fig. 1. The laser is established in an architecture which is composed of two ring cavities operating in the 1-μm and the 1.5-μm band respectively. The two cavities are attached together with a shared section comprising a 6-m-long erbium/ytterbium-codoped fiber (EYDF, Nufern SM-EYDF-

6/125-HE). The EYDF is pumped with a 975-nm laser diode (LD). The pump radiation is injected into the EYDF via a (2+1) ×1 combiner. Given that the EYDF is cladding-pumped, an in-house built cladding power stripper (CPS) is used to eliminate the residual pump in the claddings of subsequent fibers. The 1-μm cavity and the 1.5-μm cavity are separated with a 1064/1550 nm taper wavelength division multiplexer (TWDM) and a 1064/1550 nm filter wavelength division multiplexer (FWDM).

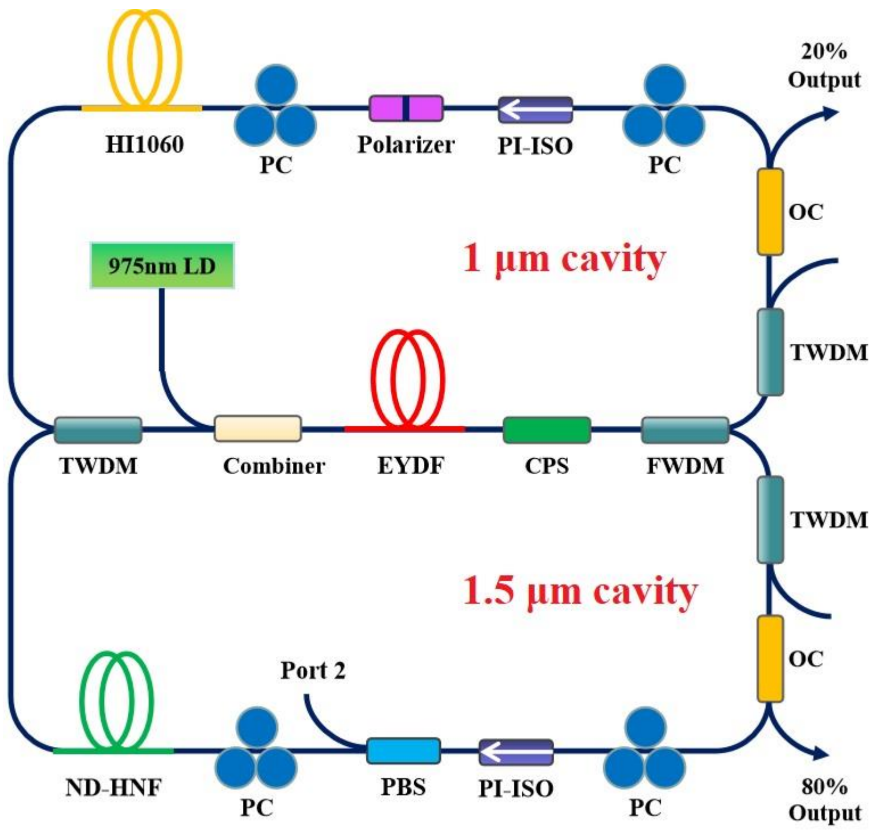

Fig. 1. Experimental setup of the 1/1.5-μm dual-band mode-locked fiber laser. EYDF: erbium/ytterbium-codoped fiber. ND-HNF: normal-dispersion high-nonlinearity fiber. LD: laser diode pump. CPS: cladding power stripper. FWDM: filter wavelength division multiplexer. TWDM: taper wavelength division multiplexer. PC: polarization controller. PI-ISO: polarization independent isolator.

The mode-locking of the 1-μm cavity is based on NPR, which is realized with a polarization-insensitive isolator (PI-ISO), a polarizer, and two polarization controllers (PCs). The 20% port of a 20:80 fiber coupler (OC) is used as the output of the 1-μm cavity. The residual 1.5-μm radiation generated in the EYDF is filtered out from the 1-μm cavity with a 1064/1550 nm TWDM. 32 m Corning HI1060 fiber is used to provide nonlinear phase shift. The pigtails of all components in the 1-μm cavity are made of HI1060 fibers. The total length of the 1-μm cavity is estimated to be 51 m. Although the 1-μm cavity exhibits all-normal dispersion, it is not necessary to use a filter to induce the mode-locking, owning to the fact that NPE behaves as an equivalent filter [23]. The 1.5-μm cavity also employs NPR as the mode-locking mechanism, which is realized with a PI-ISO, a polarization beam splitter (PBS), and two PCs. The output of the 1.5-μm cavity is performed by the 80% port of a 20:80 OC. An additional 1064/1550 nm TWDM is used to filter out the residual 1-μm radiation from the 1.5-μm cavity. A 510-m-long normal-dispersion high-nonlinearity fiber (ND-HNF) is used to provide normal dispersion in the 1.5-μm band, which render the whole cavity to exhibit a normal dispersion. The pigtail fibers of the components in the 1.5-μm cavity are either Corning SMF-28e or HI1060. The total length of the 1.5-μm cavity is estimated to be 531 m.

The Nufern EYDF plays a critical role in the dual-band operation of the laser. The fiber suffers from "bottleneck" effect as pumped with 975 nm lasers. In ordinary state an excited EYDF emits dominantly in the 1.5-μm band by exploiting the non-radiation energy transfer process between Yb^{3+} ions and Er^{3+} ions. As the bottleneck effect occurs, however, the emission in the 1 μm band increases rapidly, owing to the fact that there are too many excited Yb^{3+} ions which cannot transfer their energies to Er^{3+} ions instantly, and the energies are consequently released via the 1-μm emission. Hence, a single intensely pumped EYDF can be used as the gain medium for both the 1-μm and the 1.5-μm laser.

The output characteristics of the dual-band mode-locked fiber laser are acquired using the following equipments: optical spectrum analyzer (OSA, Yokogawa AQ6370B), oscilloscope (Tektronix DPO 7014C, bandwidth: 1 GHz), photodetector

(EOT ET-3500FEXT, bandwidth: 15 GHz), and RF spectrum analyzer (Agilent N9320A).

3. Results and discussions

In this section, we first present the experimental results of the 1.5-μm laser, given that its threshold for mode-locking is lower than the 1-μm counterpart. In the 1.5-μm cavity, the continuous wave (CW) lasing starts at a pump power of 0.6 W. As the pump power is raised to 5.94 W, initial mode-locking can be established by manipulating the PCs. Once the mode-locking is started, it can be sustained under a much lower pump power. Such an effect is well-known in NPR-based mode-locked fiber lasers [24]. In this work, we first activate the mode-locking at the threshold of 5.94 W, and then gradually reduce the pump power to search the minimal pump power that can support the mode-locking. The minimal required pump power is determined as 0.8 W. Figure 2(a) illustrates the output spectra of the 1.5-μm square-wave pulse under various pump powers. There are two prominent peaks in the spectrum that locate around the central wavelengths of 1565 nm and 1610 nm, respectively. The sharp spike on the top of the spectrum indicates that the square-wave pulse coexists with CW lasing. Figure 2(b) demonstrates the RF spectrum of the 1.5-μm laser. The repetition rate of the laser is determined as 381.3 kHz, and its RF spectral peak is of a signal-to-noise ratio (SNR) of 52 dB. The RF spectrum of the 1.5-μm laser in a 100-MHz span is presented in the inset of Fig. 2(b). A remarkable periodical modulation on the harmonics is observed. Such a modulation agrees with the square-wave nature of the 1.5-μm pulse.

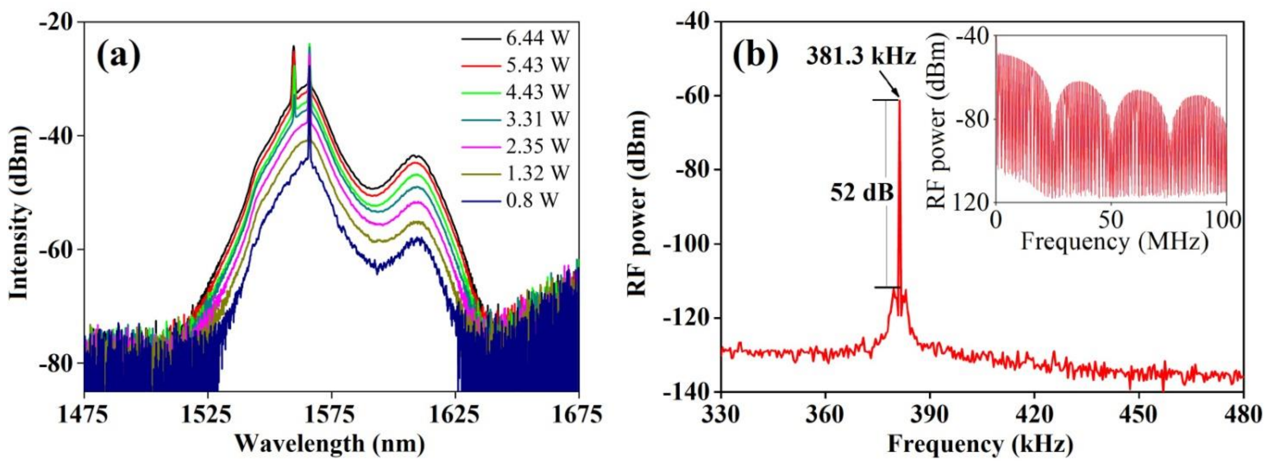

Fig. 2. (a) Evolution of the spectrum of the 1.5-μm laser with rising pump power. (b) RF spectrum of the 1.5-μm laser around the fundamental frequency. Inset: RF spectrum in a 100-MHz span.

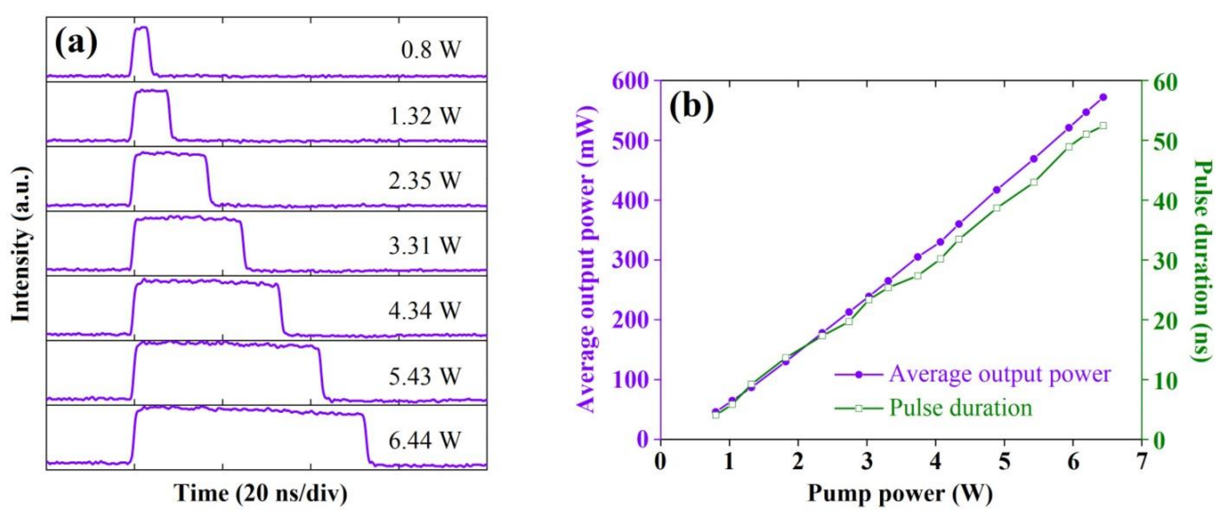

Fig. 3. (a) Evolution of the 1.5-μm square-wave pulse with rising pump power. (b) Pulse duration and average output power of the 1.5-μm laser, as functions of the pump power.

Figure 3(a) shows the evolution of the 1.5-μm pulse envelope with the rising pump power. The pulse is of a rectangular profile. As the pump power is tuned from 0.8 W to 6.44 W, the pulse duration increases from 4.05 ns to 52.43 ns, whilst the peak amplitude of the pulse almost remains constant. Figure 3(b) presents the evolution of the pulse duration and the average output power of the 1.5-μm laser as the pump power is tuned from 0.8 W to 6.44 W. It is found that the pulse duration and the output power are in a roughly linear relationship with the pump power. The output power under 6.44 W pump is 572 mW, corresponding to a pulse energy of 1.5 μJ as the 381.3 kHz repetition rate is taken into account. However, the actual pulse energy is less than the calculated value, in view of that a CW component exist in the output [see Fig. 2(a)].

In experimental works, it is found that the highest pump power to support steady fundamental mode-locking of the 1.5-μm laser is 6.44 W. As the pump power is further raised, the mode-locking become unstable. The square-wave envelope randomly splits into multi-pulses, and ultimately evolves into a second-order harmonic mode-locking, as shown in Fig. 4. The splitting of the pulse and the generation of the second-order harmonic mode-locking can be attributed to the strong nonlinear effect induced by the 510-m-long ND-HNF and the CW-lasing-related perturbation.

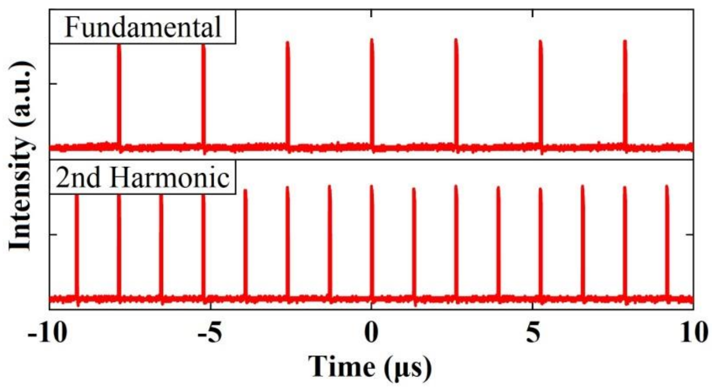

Fig. 4. Pulse trains of the fundamental and the second-order harmonic mode-locking of the 1.5-μm laser, under a pump power of 6.44 W and 8.42 W, respectively.

The threshold pump power of the 1-μm mode-locking is 6.94 W. Once the mode-locking is established, it can be sustained with a pump power as low as 6.19 W. The evolution of the output spectrum of the 1-μm laser with the rising pump power is presented in Fig. 5(a). The spectrum is of a central wavelength of ~1076 nm which almost stays invariable as the pump power is increased.

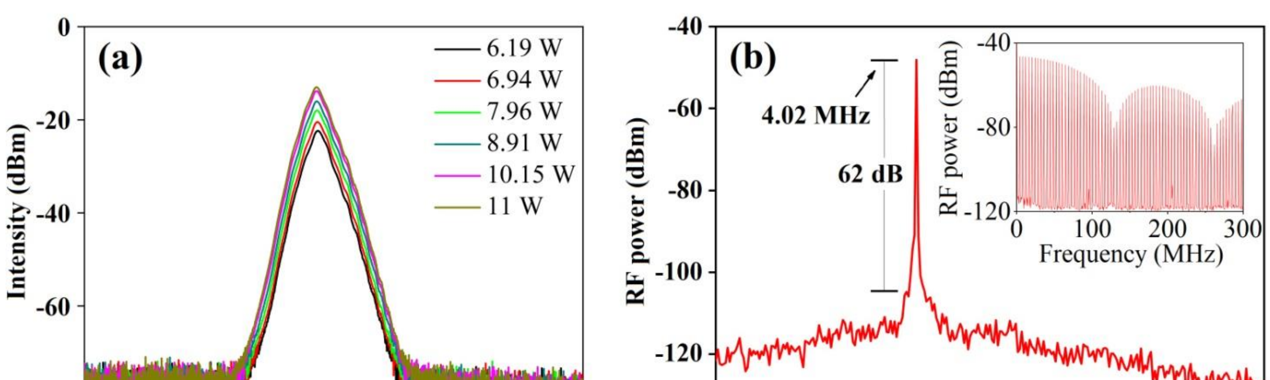

Fig. 5. (a) Evolution of the spectrum of the 1-μm laser with rising pump power. (b) RF spectrum of the 1-μm laser around the fundamental frequency. Inset: RF spectrum in a 300-MHz span.

The RF spectrum of the 1-μm laser is shown in Fig. 5(b). The fundamental frequency (i.e., the repetition rate of the laser) locates at ~4.02 MHz with a SNR of 62 dB. The inset of Fig. 5(b) shows the RF spectrum of the 1-μm laser in a 300 MHz span. The strong periodical modulation on the harmonics implies a rectangular pulse shape, which is verified by the oscilloscope trace presented in Fig. 6(a). As demonstrated in Fig. 6(a), the duration of the 1-μm square-wave pulse varies from 1.67 ns to 16.26 ns as the pump power is tuned from 6.19 W to 11 W, whilst the amplitude of the pulse remains almost the same. Figure 6(b) illustrates the evolution of the pulse duration and the average output power of the 1-μm laser through the rising pump power. The relationship between the pulse duration (and average output power) and the pump power of the 1-μm laser is nonlinear. Such a nonlinear relationship can be attributed to the influence of the second-order harmonic mode-locking of the 1.5-μm laser. The maximum output power of the 1-μm laser achieved in the experimental works is 356 mW. The highest pulse energy of the 1-μm pulse is accordingly determined to be 88.6 nJ, as the 4.02 MHz repetition rate is taken into account.

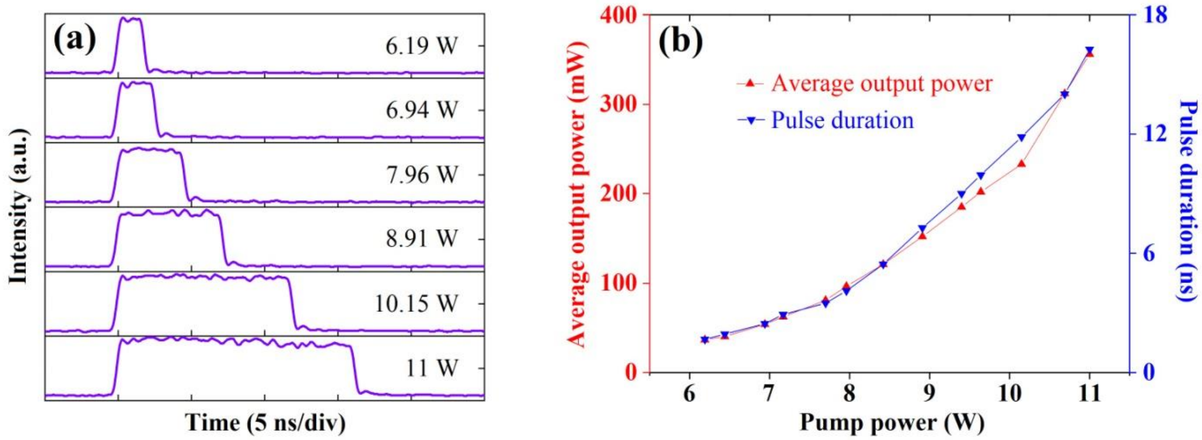

Fig. 6. (a) Evolution of the 1-μm square-wave pulse with rising pump power. (b) Pulse duration and average output power of the 1-μm laser, as functions of the pump power.

4. Conclusions

In this paper, we experimentally demonstrate a 1/1.5-μm dual-band simultaneously mode-locked fiber laser. The laser generates high-energy, square-wave pulses in both the 1-μm band and the 1.5-μm band. The 1-μm pulse achieves an energy of 88.6 nJ with a repetition rate of 4.02 MHz. The 1.5-μm pulse achieves an energy up to 1.5 μJ with a repetition rate of 381.3 kHz. Both the 1-μm pulse and the 1.5-μm pulse experiences a wave-breaking-free increase of the pulse duration as the power is raised, whilst the 1.5-μm pulse split and ultimately evolves into higher-order mode-locking as the pump power is beyond a certain value. The laser, with its capacity to generate high-energy square-wave pulses in two spectral bands, can be potential tools for many applications.

Acknowledgement

This work was supported by the National Natural Science Foundation of China (NSFC) (61975136, 61935014, 61775146, 61905151); Outstanding Young Teacher Cultivation Projects in Guangdong Province (YQ2015142); Guangdong Basic and Applied Basic Research Foundation (2019A1515010699); Shenzhen Science and Technology Project (JCYJ20160520161351540, JCYJ20170817100639177, JCYJ20170302151146995, JCYJ20160328144942069); Engineering Applications of Artificial Intelligence Technology Laboratory Project (PT201701).

References:

[1] P. Li, A. Ruehl, U. Grosse-Wortmann, and I. Hartl, "Sub-100 fs passively mode-locked holmium-doped fiber oscillator operating at 2.06 μm," *Opt. Lett.*, vol. 39, no. 24, pp. 6859–6862, 2014.

[2] F. Chen, Q. Hao, and H. Zeng, "Optimization of an NALM mode-locked all-PM Er:fiber laser system," *IEEE Photon. Technol. Lett.*, vol. 29, no. 23, pp. 2119–2122, 2017.

[3] R. Song, H. W. Chen, S. P. Chen, J. Hou, and Q. S. Lu, "A SESAM passively mode-locked fiber laser with a long cavity including a band pass filter," *J. Opt.*, vol. 13, no. 3, pp. 035201, 2011.

[4] X. T. Xu, J. P. Zhai, L. Li, Y. P. Chen, Y. Q. Yu, M. Zhang, S. C. Ruan, and Z. K. Tang, "Passively mode-locking erbium-doped fiber lasers with 0.3 nm Single-Walled Carbon Nanotubes," *Sci. Rep.*, vol. 4, pp. 6761, 2014.

[5] P. G. Yan, R. Y. Lin, H. Chen, H. Zhang, A. J. Liu, H. P. Yang, and S. C. Ruan, "Topological insulator solution filled in photonic crystal fiber for passive mode-locked fiber laser," *IEEE Photon. Technol. Lett.*, vol. 27, no. 3, pp. 264–267, 2015.

[6] P. G. Yan, R. Y. Lin, S. C. Ruan, A. J. Liu, and H. Chen, "A 2.95 GHz, femtosecond passive harmonic mode-locked fiber laser based on evanescent field interaction with topological insulator film," *Opt. Express*, vol. 23, no. 1, pp. 154–164, 2015.

[7] Y. Chen, M. Wu, P. Tang, S. Chen, J. Du, G. J, Y. Li, C. Zhao, H. Zhang, and S. Wen, "The formation of various multi-soliton patterns and noise-like pulse in a fiber laser passively mode-locked by a topological insulator based saturable absorber," *Laser Phys. Lett.*, vol. 11, pp. 055101, 2014.

[8] J. Li, H. Luo, B. Zhai, R. Lu, Z. Guo, H. Zhang, and Y. Liu, "Black phosphorus: a two-dimension saturable absorption material for mid-infrared Q-switched and modelocked fiber lasers," *Sci. Rep.*, vol. 6, pp. 30361, 2016.

[9] K. Yin, B. Zhang, W. Yang, H. Chen, S. Chen, Shengping, and J. Hou, "Flexible picosecond thulium-doped fiber laser using the active mode-locking technique," *Opt. Lett.*, vol. 39, no. 14, pp. 4259–4262, 2014.

[10] K. Krzempek, G. Sobon, and K. M. Abramski, “DFG-based mid-IR generation using a compact dual-wavelength all-fiber amplifier for laser spectroscopy applications,” *Opt. Express*, vol. 21, no. 17, pp. 20023–20031, 2013.
[11] F. Ganikhanov, S. Carrasco, X. S. Xie, M. Katz, W. Seitz, and D. Kopf, “Broadly tunable dual-wavelength light source for coherent anti-Stokes Raman scattering microscopy,” *Opt. Lett.*, vol. 31, no. 9, pp. 1292–1294, 2006.
[12] M. Rusu, R. Herda, and O. G. Okhotnikov, “Passively synchronized erbium (1550-nm) and ytterbium (1040-nm) mode-locked fiber lasers sharing a cavity,” *Opt. Lett.*, vol. 29, no. 19, pp. 2246–2248, 2004.
[13] M. Zhang, E. J. R. Kelleher, A. S. Pozharov, E. D. Obraztsova, S. V. Popov, and J. R. Taylor, “Passive synchronization of all-fiber lasers through a common saturable absorber,” *Opt. Lett.*, vol. 36, no. 20, pp. 3984–3986, 2011.
[14] J. Sotor, G. Sobon, I. Pasternak, A. Krajewska, W. Strupinski, and K. M. Abramski, “Simultaneous mode-locking at 1565 nm and 1944 nm in fiber laser based on common graphene saturable absorber,” *Opt. Express*, vol. 21, no. 16, pp. 18994–19002, 2013.
[15] L. E. Nelson, D. J. Jones, K. Tamura, H. A. Haus, and E. P. Ippen, “Ultrashort-pulse fiber ring lasers,” *Appl. Phys. B*, vol. 65, no. 2, pp. 277–294, 1997.
[16] K. Tamura, E. P. Ippen, H. A. Haus, and L. E. Nelson, “77-fs pulse generation from a stretched-pulse mode-locked all-fiber ring laser,” *Opt. Lett.*, vol. 18, no. 13, pp. 1080–1082, 1993.
[17] D. Mortag, D. Wandt, U. Morgner, D. Kracht, and J. Neumann, “Sub-80-fs pulses from an all-fiber-integrated dissipative-soliton laser at 1 µm,” *Opt. Express*, vol. 19, no. 2, pp. 546–551, 2011.
[18] J. R. Buckley, F. W. Wise, F. Ö. Ilday, and T. Sosnowski, “Femtosecond fiber lasers with pulse energies above 10 nJ,” *Opt. Lett.*, vol. 30, no. 14, pp. 1888–1890, 2005.
[19] X. Zhang, C. Gu, G. Chen, B. Sun, L. Xu, A. Wang, and H. Ming, “Square-wave pulse with ultra-wide tuning range in a passively mode-locked fiber laser,” *Opt. Lett.*, vol. 37, no. 8, pp. 1334–1336, 2012.
[20] Y. Xu, Y. L. Song, G. G. Du, P. G. Yan, C. Y. Guo, G. L. Zheng, and S. C. Ruan, “Dissipative soliton resonance in a wavelength-tunable thulium-doped fiber laser with net-normal dispersion,” *IEEE Photon. J.*, vol. 7, no. 3, pp. 1502007, 2015.
[21] H. Q. Lin, C. Y. Guo, S. C. Ruan, and J. H. Yang, “Dissipative soliton resonance in an all-normal-dispersion Yb-doped figure-eight fibre laser with tunable output,” *Laser Phys. Lett.*, vol. 11, no. 8, pp. 085102, 2014.
[22] J. H. Yang, C. Y. Guo, S. C. Ruan, D. Q. Ouyang, H. Q. Lin, Y. M. Wu, and R. H. Wen, “Observation of dissipative soliton resonance in a net-normal dispersion figure-of-eight fiber laser,” *IEEE Photon. J.*, vol. 5, no. 3, pp. 1500806, 2013.
[23] L. Zhao, D. Tang, X. Wu, and H. Zhang, “Dissipative soliton generation in Yb-fiber laser with an invisible intracavity bandpass filter,” *Opt. Lett.*, vol. 35, no. 16, pp. 2756–2758, 2010.
[24] C.-J. Chen, P. K. A. Wai, and C. R. Menyuk, “Self-starting of passively mode-locked lasers with fast saturable absorbers,” *Opt. Lett.* vol. 20, no. 4, pp. 350–352, 1995.